BJP British Journal of Pharmacology

DOI:10.1111/bph.12207
www.brjpharmacol.org

RESEARCH PAPER

Pathway specific modulation of S1P1 receptor signalling in rat and human astrocytes

Luke M Healy[1], Graham K Sheridan[1], Adam J Pritchard[1], Aleksandra Rutkowska[1], Florian Mullershausen[2] and Kumlesh K Dev[1]

[1]*Molecular Neuropharmacology, Department of Physiology, School of Medicine, Trinity College Institute of Neuroscience, Trinity College Dublin, Dublin, Ireland, and* [2]*Novartis Institutes for BioMedical Research, Novartis Pharma AG, Basel, Switzerland*

Correspondence
Professor Kumlesh K Dev, Molecular Neuropharmacology, Department of Physiology, School of Medicine, Trinity College Institute of Neuroscience, Trinity College Dublin, Dublin 2, Ireland. E-mail: devk@tcd.ie

Keywords
sphingosine 1-phosphate receptor subtype 1 (S1P1R); *p*FTY720; astrocytes; receptor signalling; Multiple Sclerosis (MS)

Received
9 September 2012
Revised
9 March 2013
Accepted
21 March 2013

BACKGROUND AND PURPOSE

The sphingosine 1-phosphate receptor subtype 1 (S1P1R) is modulated by phosphorylated FTY720 (*p*FTY720), which causes S1P1R internalization preventing lymphocyte migration thus limiting autoimmune response. Studies indicate that internalized S1P1Rs continue to signal, maintaining an inhibition of cAMP, thus raising question whether the effects of *p*FTY720 are due to transient initial agonism, functional antagonism and/or continued signalling. To further investigate this, the current study first determined if continued S1P1R activation is pathway specific.

EXPERIMENTAL APPROACH

Using human and rat astrocyte cultures, the effects of S1P1R activation on cAMP, pERK and Ca^{2+} signalling was investigated. In addition, to examine the role of S1P1R redistribution on these events, a novel biologic (MNP301) that prevented pFTY720-mediated S1P1R redistribution was engineered.

KEY RESULTS

The data showed that *p*FTY720 induced long-lasting S1P1R redistribution and continued cAMP signalling in rat astrocytes. In contrast, *p*FTY720 induced a transient increase of Ca^{2+} in astrocytes and subsequent antagonism of Ca^{2+} signalling. Notably, while leaving pFTY720-induced cAMP signalling intact, the novel MNP301 peptide attenuated S1P1R-mediated Ca^{2+} and pERK signalling in cultured rat astrocytes.

CONCLUSIONS AND IMPLICATIONS

These findings suggested that *p*FTY720 causes continued cAMP signalling that is not dependent on S1P1R redistribution and induces functional antagonism of Ca^{2+} signalling after transient stimulation. To our knowledge, this is the first report demonstrating that *p*FTY720 causes continued signalling in one pathway (cAMP) versus functional antagonism of another pathway (Ca^{2+}) and which also suggests that redistributed S1P1Rs may have differing signalling properties from those expressed at the surface.

Introduction

The family of sphingosine 1-phosphate receptors (S1PRs) are G protein-coupled comprising five subtypes (S1P1R–S1P5R) (Dev *et al.*, 2008). These receptors are expressed in cells of the immune, cardiovascular and CNS, in addition to others. S1PRs play important roles in cellular proliferation, differentiation, survival and migration (Dev *et al.*, 2008). The immunomodulatory drug, Gilenya® has been approved as the first oral therapy for multiple sclerosis (MS), after proving efficacious in clinical trials (Kappos *et al.*, 2010). The active ingredient of Gilenya is the phosphorylated compound FTY720 (*p*FTY720), which is a potent agonist on all S1PRs, except S1P2Rs (Brinkmann *et al.*, 2002). *p*FTY720 has been suggested to work as a 'functional antagonist' causing S1P1R internalization in lymphocytes, thus limiting T cell auto-immunity

(Brinkmann *et al.*, 2002; Goetzl and Graler, 2004). In addition to regulating the immune system, the lipophilic nature of the pro-drug FTY720 allows it to readily cross the blood-brain-barrier (Meno-Tetang *et al.*, 2006), where the *p*FTY720 form may also activate S1PRs expressed on both neurons and glia.

Previous studies show that S1PRs play roles in (i) astrocyte signalling and migration, (ii) oligodendrocyte differentiation, process retraction and survival and (iii) neurite outgrowth, axonal guidance, synaptic excitability, and neurogenesis (Dev *et al.*, 2008). In astrocytes, S1PR activation regulates many intracellular signalling events, including an increase in intracellular Ca^{2+} levels, inhibition of adenylyl cyclase to decrease cAMP levels, activation of phospholipase A2 to produce arachadonic acid and activation of phospholipase C to induce phospho-inositide hydrolysis (Pebay *et al.*, 2001; Sorensen *et al.*, 2003; Mullershausen *et al.*, 2007; Osinde *et al.*, 2007). S1PR activation also increases the non-phosphorylated levels of Connexin 43, which may play a role in neuronal survival (Rouach *et al.*, 2006). Studies have also found that activation of S1PRs stimulates astrocyte proliferation *in vitro* and in mouse brain (Pebay *et al.*, 2001; Malchinkhuu *et al.*, 2003; Rao *et al.*, 2003; Sorensen *et al.*, 2003; Yamagata *et al.*, 2003; Bassi *et al.*, 2006). In Sandhoff disease mice (a neurodegenerative lysosomal storage disorder), the deletion of S1P3Rs reduces astrogliosis and disease course indicating this receptor subtype may play a major role in astrocyte proliferation (Wu *et al.*, 2008). Astrocytes migrate towards injury sites in spinal cord where they release S1P, which promotes migration of neural stem cells that is thought to be important for repair (Kimura *et al.*, 2007). Additionally, S1P promotes the release of growth factors (NGF, FGF-2 and GDNF) from astrocytes that can allow for cellular crosstalk and promote neuronal survival (Sato *et al.*, 1999; Riboni *et al.*, 2001; Malchinkhuu *et al.*, 2003; Yamagata *et al.*, 2003; Bassi *et al.*, 2006; Furukawa and Furukawa, 2007). Following traumatic brain injury, *p*FTY720 reduces IL-16 levels in astrocytes (and microglia and neurons), which is also likely to be important for crosstalk with cells of the immune system (Zhang *et al.*, 2008). It has also been shown that increases in IL-1β, IL-6 and IL-17 in animal models of experimental allergic encephalomyelitis (EAE) are attenuated by specific S1P1R knockout from astrocytes or *p*FTY720 treatment, lending strong support for a role of S1P1R in astrocytes in EAE (Choi *et al.*, 2011).

The suggestion that internalization and thus functional antagonism of S1P1Rs is a mechanism by which *p*FTY720 is protective in MS has also been supported in an elegant study showing that specific abilation of S1P1Rs is protective in an animal model of EAE (Choi *et al.*, 2011). Given that the study specifically knocked-out S1P1Rs from astrocytes, a role of astrocyte expressed S1P1Rs in the development EAE and effectiveness of *p*FTY720 was also suggested (Choi *et al.*, 2011). The functional consequences of ligand-induced internalization of the S1P1R in HUVECs has also been reported (Mullershausen *et al.*, 2009). In that study, *p*FTY720 induced long-term S1P1R internalization and inhibition of adenylyl cyclase several hours after washout of the drug (Mullershausen *et al.*, 2009). Taken together, these reports raise an important question whether the effects of *p*FTY720 are due to transient initial agonism, functional antagonism and/or continued signalling. In order to investigate this question, here, the pathway specific and long-lasting effects of *p*FTY720 on cAMP, pERK and Ca^{2+} signalling was examined in astrocytes.

Materials and methods

Compounds and antibodies

All experiments used the pure active (S)-enantiomer of *p*FTY720 (2-amino-2-[2-(4-octylphenyl)ethyl] propane-1,3-diol). The SEW2871 compound (Calbiochem, Boston, MA, USA) and AUY954 (Novartis Pharma, Basel, Switzerland) were used as S1P1R selective agonists. S1P (Enzo Life Sciences, Ann Arbor, MI, USA) was prepared as a 5 mM stock solution in DMSO with 50 mM HCl. Primary antibodies were polyclonal rabbit anti-S1P1R (Santa Cruz, Dallas, TX, USA, sc-25489), anti-p44/42 MAP Kinase (cat #9102, Cell Signaling, Danvers, MA, USA) and anti-phospho-p44/42 MAP Kinase (Cell Signaling) and mouse monoclonal antibodies, anti-GFAP (Millipore, USA, MAB360), anti-beta Actin (clone AC15, cat # A1978, Sigma-Aldrich, St. Louis, MO, USA), anti-EEA1 (BD Biosciences, Franklin Lakes, NJ, USA, 610457), anti-GM130 (BD Biosciences, 610822), anti-LAMP1 (BD Biosciences, 555798), anti-p230 (BD Biosciences, 611280). Secondary antibodies utilized were peroxidase conjugated (HRP) goat anti-mouse or anti-rabbit IgG (Sigma), biotinylated goat anti-rabbit IgG (Vector, Peterborough, UK, BA1000), streptavidin conjugated Alexa 488 and 633 (Invitrogen, Grand Island, NJ, USA, S11223 and S2137), Alexa Fluor 488 goat anti-mouse (Invitrogen, A1101), Alexa Fluor 633 goat anti-mouse (Invitrogen, A21050). Nuclear stain Hoechst 34580 (Invitrogen, H21486).

Culture of primary astrocytes

Primary cortical astrocyte cultures were prepared using post-natal day one Wistar rats of either sex (Bioresources Unit, Trinity College Dublin), in accordance with the Animals Act 1986 (Scientific Procedures) Schedule I guidelines. Briefly, the brain was freed of meninges and cortices were dissected in warmed DMEM/F12 (Biosera, East Sussex, UK), supplemented with 10% heat inactivated FBS (Biosera) and 1% penicillin/streptomycin (100 $\mu L \cdot mL^{-1}$; Invitrogen) (sDMEM). Tissue was incubated in sDMEM/F12 for 20 m at 37°C, the tissue was triturated and passed through a sterile nylon mesh cell strainer (40 μm; BD Biosciences). Cell filtrate was centrifuged and the pellet resuspended in sDMEM/F12. Cells were plated on poly-L-lysine (40 $\mu g \cdot mL^{-1}$ in sterile H_2O: Sigma Aldrich, Germany) coated T75 culture flasks (Cat #83.1813.002, Sarstedt AG, Nümbrecht, Germany). When confluent the flasks were shaken at 200 rpm for 3 h at 37°C in an orbital shaker (Excella E24, New Brunswick Scientific, Boulevard Enfield, CT, USA) and non-astrocyte cells removed. The astrocyte layer was incubated with 0.1% trypsin-EDTA in serum free DMEM/F12 for 20 m at 37°C, sDMEM/F12 was added to the flasks to inhibit the trypsin. The cell suspension was collected, centrifuged and resuspended in 8 mL sDMEM/F12 and plated at a density of 1×10^5 $cells \cdot mL^{-1}$ on borosilicate glass coverslips pre-coated with poly-L-lysine in 24-well plates. Primary astrocytes were maintained at 37°C in a humidified incubator supplied with 5% CO_2. Cells were grown until confluent and were starved in serum-free media for 3 h prior to treatment.

SDS-PAGE and Western blotting

Samples were denatured and electrophoresis carried out on 10% SDS-polyacrylamide gels. Semi-dry electrophoretic blotting was performed using polyvinylidene difluoride microporous membrane (PVDF, Immobilon P, Millipore). The PVDF membrane was then (i) blocked, (ii) incubated with primary antibody, (iii) washed, (iv) incubated with HRP conjugated secondary antibody, and (v) washed again before (vi) exposing to development reagent. All blocking and antibody incubation steps were performed in PBST-block (PBS, 0.1% Tween-20 supplemented with 5% non-fat milk) for 1 h at room temperature and all wash steps performed by 3 × 5 min incubation with PBST. Blots were developed by incubating in Immobolin chemiluminescent HRP substrate and imaged on a Fujifilm LAS-3000 Intelligent Dark-box. Densitometry measurement of band intensity was used for quantification (MCID Elite, InterFocus Imaging Ltd, Cambridge, UK).

Cell surface biotinylation

Non-permeable biotin (Sulfo NHS-LC-Biotin; ProteoChem, Cheyenne, WY, USA) was used to identify cell surface-expressed membrane proteins. Cultured human astrocytes were serum starved for 4 h, pretreated with or without 100 μg·mL^{-1} MNP301 for 1 h and then incubated with or without 1 μM pFTY720 for 1 h. Astrocytes were then incubated with 0.5 mg·mL^{-1} biotin for 30 min at 4°C, after which the cells were scraped in PTxE buffer (PBS, 1% Triton X-100, 0.1 mM EDTA, pH 7.4) at 4°C. The cell suspension was then sonicated for 10 × 2 s (Astrason). Sonicates were solubilized by rotation for 1 h at 4°C in ice-cold PTxE buffer and then centrifuged at 21 100× *g* for 20 min in a microfuge to remove cell debris. The cell sonicate was removed for immunoprecipitation. Sample biotin was immunoprecipitated for 2 h at 4°C using streptavidin-coated agarose beads (Sigma), then analysed by Western blotting.

Adenylate cyclase assay

Astrocytes were trypsinized, diluted and seeded into 24-well cell culture plates (MidSci, Saint Louis, MO, USA) at a cell density of 5×10^5 cells·mL^{-1}. Cells were left for 2–3 days before assaying for cAMP levels, as previously described (Salomon, 1979). Briefly, cells were incubated in 500 μL of serum free DMEM/F12 for 3 h at 37°C/5% CO_2 before use. Cells were then loaded with [H^3] adenine in serum free media for 4 h at 37°C/5% CO_2 and then washed with PBS supplemented with $CaCl_2$ (0.9 mM) and $MgCl_2$ (0.5 mM). Stimulations were carried out in Hank's balanced salt solution (HBSS; Invitrogen) with 20 μM forskolin (Sigma-Aldrich, Munich, Germany). Stimulation were carried out in the presence of the phosphodiesterase inhibitors 1 mM IBMX (3-isobutyl-1-methylxanthine; Enzo Life Sciences), 10 μM Rolipram (Enzo Life Sciences) and 1 μM BAY 60–7550 (Enzo Life Sciences) to inhibit degradation of cAMP. Cells were treated either with 1 μM *p*FTY720 for 20 min to determine immediate effects on cAMP levels, or treated with 1 μM *p*FTY720 for 1 h followed by a 5-h washout period to determine effects on persistent signalling. Cells were also pre-incubated with or without 100 μg·mL^{-1} MNP301 for 1 h, prior to addition of *p*FTY720. The cAMP experiments were carried out by washing the cells directly prior to testing for Gi-cAMP.

Calcium signalling

Cells were grown until ~80% confluencey on poly-d-lysine coated, glass bottomed, 35 mm FluoroDishes (World Precision Instruments, Sarasota, FL, USA). Cells were pretreated with S1PR agonists in serum free DMEM/F12 for 1 h. Cells were then washed twice in serum free media and left in fresh serum free media for 3 h. Cells were washed once with 1 mL 37°C HBSS (Invitrogen) supplemented with 20 mM HEPES buffer (Invitrogen) and 5.5 mM glucose (Sigma Aldrich). Cells were then loaded with 2 μM Fluo-4 AM (Invitrogen) in supplemented 37°C HBSS for 20mins at 37°C and 5% CO2. Fluo-4 AM dye was removed and cells were washed once with 37°C supplemented HBSS. Next, cells were left to rest in 1 mL supplemented HBSS at room temperature in the dark for 20 min. Calcium responses were recorded using a Zeiss LSM 510 META confocal laser scanning microscope (Zeiss Ltd, Cambridge, UK), scanning speed was 1 frame·s^{-1}. Stimulation of cells was performed by adding a three times concentrated solution of test reagent in supplemented HBSS with a manual pipette. Baseline recordings were taken for 30 s, test reagents were then added and changes in $_iCa^{2+}$ levels were recorded for a further 150 s. After 180 s, 30 μM glutamate (Sigma Aldrich) was added and recording was continued for a further 60 s. Recordings were terminated at 240 s.

Immunocytochemistry

Cells were fixed in ice-cold 100% methanol for 10 min followed by permeabilization with 0.2% Triton-X-100 (Sigma Aldrich) in PBS for 5 min at room temperature. Non-reactive sites were blocked overnight at 4°C with 10% normal goat serum (Invitrogen) and 2% BSA (Sigma Aldrich) in PBS. Cells were incubated in primary antibody overnight at 4°C. Primary antibody was removed and cells washed 3 × 5 m PBS followed by incubation with a biotin conjugated secondary antibody (Vector) for 2 h at room temperature. Wash steps were repeated and cells were incubated with avidin-Alexa antibody for 45 min. Cells were counter stained with Hoescht 34580 nuclear stain and mounted on microscope slides in Vectashield mounting medium (Vector), the edges of the coverslips were sealed with nail varnish. Cells were imaged using a Zeiss LSM 510 META confocal laser scanning microscope utilizing an Axiovert 200 M inverted microscope (Zeiss Ltd). Images were captured and optimized using LSM510 computer software.

Image analysis and quantification

Image analysis was carried out using the bioconductor package, EBImage (http://www.bioconductor.org/packages/release/bioc/html/EBImage.html), for the R statistical programming environment. Briefly, red, green and blue channels were separated for each image and every pixel within the images (1024 × 1024) was assigned an intensity value between 0 and 1. Blue channel represents Hoechst-stained nuclei and red channel GFAP-labelled astrocytic processes. Both channels were used to label the nuclear, perinuclear and cytoplasmic compartments of the astrocyte cells. An analysis script was written in R to measure the fluorescence intensity of S1P1R staining (i.e. green channel) in each of these three-distinct cellular compartments in all cells within the confocal images. Using the blue (Hoechst) channel, minimum size and

fluorescence intensity thresholds were set in order to select only those pixels that belong to Hoechst-labelled nuclei. The nuclei were then 'dilated' using specified morphological kernel expansion. This step allowed the designation of a perinuclear region surrounding each nucleus. The nuclear and perinuclear compartments of each cell were then subtracted from the red channel and the remaining GFAP-labelled processes were used to calculate the average fluorescence intensity of S1P1Rs in the cytoplasmic compartment of astrocytes within each image. A distance map was then generated for the image which calculates the distance each pixel is from an edge pixel. The watershed segmentation algorithm accurately separates nuclei that are very close together or touching. The perinuclear-to-cytoplasmic fluorescence intensities of each cell were calculated according to the equation [Fp/Fc], where Fp = average perinuclear fluorescence and Fc = average cytoplasmic fluorescence. Increases in the Fp : Fc ratio measures increased S1P1R internalization and trafficking of the receptor from astroctytic processes to the perinuclear compartment of the cell.

Results

p*FTY720 induces redistribution of the S1P1R in rat astrocytes*

Before investigating the effects of *p*FTY720 on S1P1R redistribution and cellular localization, the purity of primary rat astrocyte cultures was assessed using antibodies (Abs) against markers of astrocytes (GFAP), neurons (neurofilament H), microglia (CD11b) and oligodendrocytes (CNPase) and the Hoechst nuclear stain to determine the total cell count. GFAP positive cells were expressed as a percentage of total cell counts and were found to be greater than 98% pure, in agreement with previous studies (Mullershausen *et al.*, 2007; Osinde *et al.*, 2007) (Figure 1A). The expression of S1P1Rs under control conditions was also confirmed in astrocytes as determined by co-localization of S1P1R and GFAP immunoreactivity (Figure 1B). Next, astrocytes were treated with increasing concentrations of *p*FTY720 for 1 h at 37°C and cells were immunostained with anti-S1P1R (green) and anti-GFAP (red) Abs. Treatment with *p*FTY720 caused redistribution of the S1P1R subtype to a peri-nuclear compartment, as shown by confocal microscopy (Figure 1B). Increasing concentrations of *p*FTY720 caused increasing levels of redistributed S1P1R, that was evident at both 100 nM and 1 μM *p*FTY720 (Figure 1B). To investigate the kinetics of this S1P1R redistribution, the effects of 1 μM *p*FTY720 were measured at different time points. Increasing drug treatment times caused increasing levels of S1P1R redistribution (Figure 1C). Effective redistribution was observed partially after 30 min treatment with *p*FTY720 and was clearly evident after 1 h drug treatment (Figure 1C) and remained after 4-h treatment (not shown, however see Figure 2A).

S1P1Rs display redistibution toward the TGN in astrocytes

Following previous observations that *p*FTY720 causes rapid and long-lasting internalization of the S1P1R subtype in CHO cells stably expressing S1P1R and in primary HUVECs expressing endogenous S1P1R (Mullershausen *et al.*, 2009), this event was investigated in primary rat astrocyte cells. Astrocytes treated with *p*FYT720 (1 μM) for 1 h at 37°C caused S1P1R redistribution to a peri-nuclear region as described above (Figure 2A). Moreover, under conditions of *p*FTY720 treatment (1 μM) for 1 h at 37°C, followed by a 5-h washout period, the S1P1R remained localized in a punctate manner (Figure 2A), which in some cases was more prominent than after 1 h *p*FTY720 treatment. In agreement, automated image analysis showed a significant increase in the ratio of S1P1R redistribution between the vehicle control and both the 1 h *p*FTY720 treatment group and the 5-h washout group (Figure 2B**,** C). To examine the localization of the redistributed S1P1Rs, astrocytes treated with *p*FTY720 (1 μM) for 1 h at 37°C were stained with various organelle markers. Staining with the early endosome marker (EEA-1) showed no colocalization with the redistributed S1P1R (Figure 2D). In addition, counter staining with the lysosome marker (LAMP1) also showed minimal co-localization with the redistributed pool of S1P1Rs (Figure 2D). In contrast, the data showed considerable overlap of S1P1R staining with both markers for the trans-Golgi-network (TGN) (p230) and the Golgi complex (GM130) (Figure 2D). To determine the specificity of ligand-induced redistribution of the S1P1R, the effects of the endogenous ligand S1P and a synthetic S1P1R-selective agonist SEW2871 were examined in primary astrocyte cultures. Automated image analysis showed that 1 h treatment of either 1 μM *p*FTY720 or 1 μM SEW2871 caused significant redistribution of S1P1R compared to vehicle control (Figure 2E). In contrast, the endogenous ligand 1 μM S1P caused no change in S1P1R cellular localization after a 1-h treatment (Figure 2E).

MNP301 prevents p*FTY720 induced redistribution of S1P1R*

The carboxy termal (ct) of receptors can interact with trafficking proteins that regulate receptor cycling and these interactions can be prevented by competitive blocking peptides, for example as that found for glutamate receptors (Dev *et al.*, 2000). Based on this hypothesis, in order to uncouple the agonist effects of *p*FTY720 from its effects on S1P1R cellular localization, a biologically active peptide (MNP301) that prevents *p*FTY720-mediated redistribution of S1P1R was engineered. Specifically, MNP301 was modelled on the last 10 residues of ct-S1P1R, fused to a protein transduction domain based on the HIV trans-activating transcriptional activator (Tat) sequence for cell delivery and labelled with FITC for visulization inside the cell (FITC-Ahx-YGRKKRRQRRR-MSSGNVNSSS) (Figure 3A). Primary rat astrocyte cultures were treated with increasing concentrations of MNP301 for 1 h at 37°C and cells were washed prior to fixation to remove any non-specific bound MNP301. Confocal microscopy and automated image analysis showed that MNP301 transduced astrocytes in a concentration-dependant manner (Figure 3B). Significant cellular transduction was observed following incubation of astrocytes with 100 $\mu g \cdot mL^{-1}$ MNP301 compared to control (Figure 3B). To further confirm cellular transduction organotypic cerebellar cultures were prepared as described previously (Sheridan and Dev, 2012) and treated acutely for 2 h with MNP301, then placed into fresh medium for a further 2 days. The slices were then stained for S1P1R

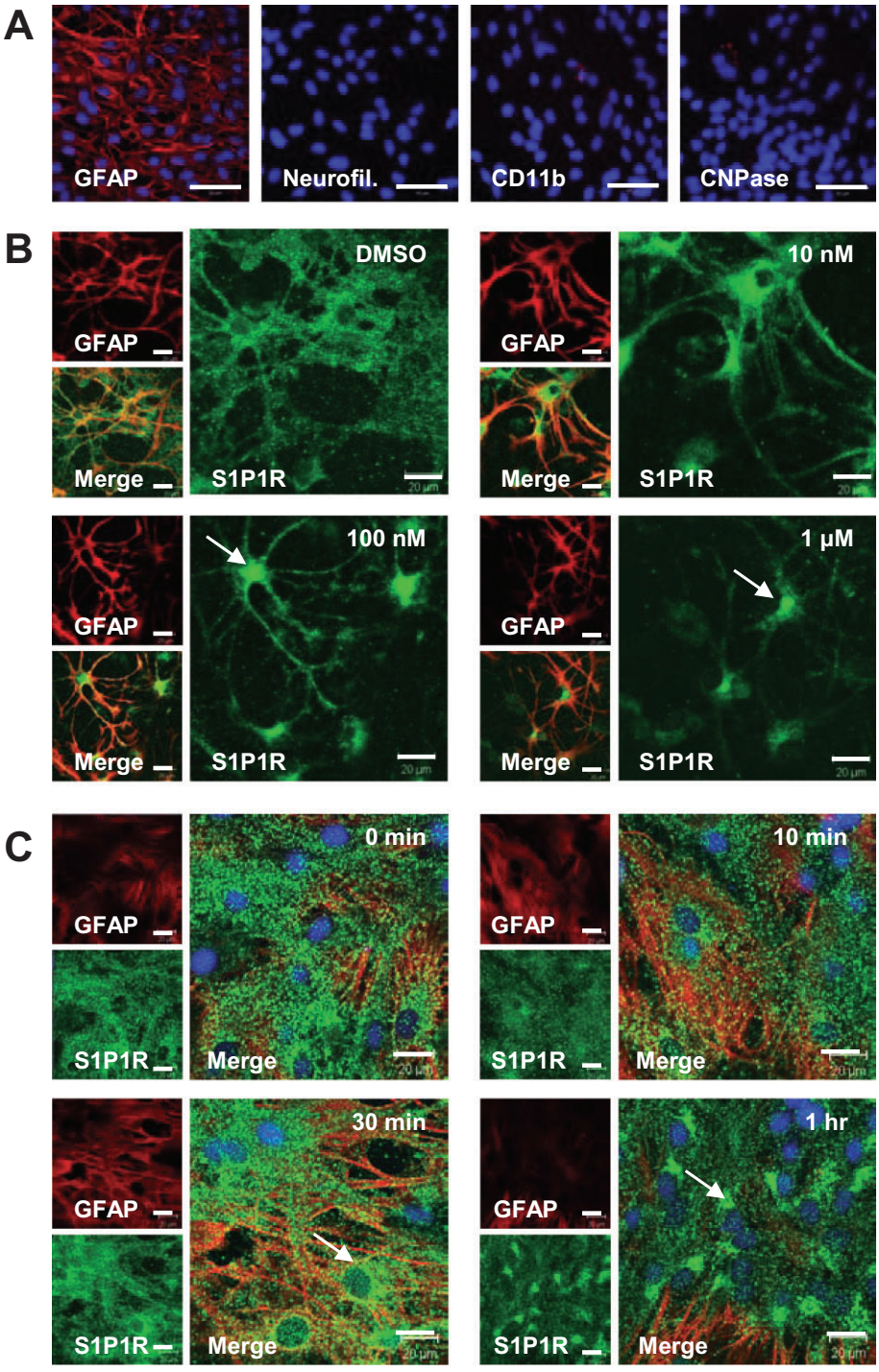

Figure 1

pFTY720 treatment causes redistribution of S1P1R in a time and concentration dependent manner in astrocytes. (A) Pure rat astrocytes were stained for GFAP, neurofilament H, CD11b and CNPase. A total of 24 images were analysed (six images per group). Average percentage of positively stained cells for each group was as follows: GFAP 98.58% ± 0.57, CD11b 1.35% ± 0.77 and CNPase 1.83% ± 0.48. No neurofilament H positive cells were observed. Scale bars 50 µm. Pure astrocyte cultures were treated with (B) increasing concentrations of *p*FTY720 for 1 h or (C) with 1 µM *p*FTY720 for time periods indicated. Unless indicated, cells were immunostained with GFAP Ab (red) and S1P1R Ab (green), cell nuclei appear as blue (Hoescht) and arrows indicate areas of S1P1R redistribution as determined by perinuclear staining. Scale bars 20 µm.

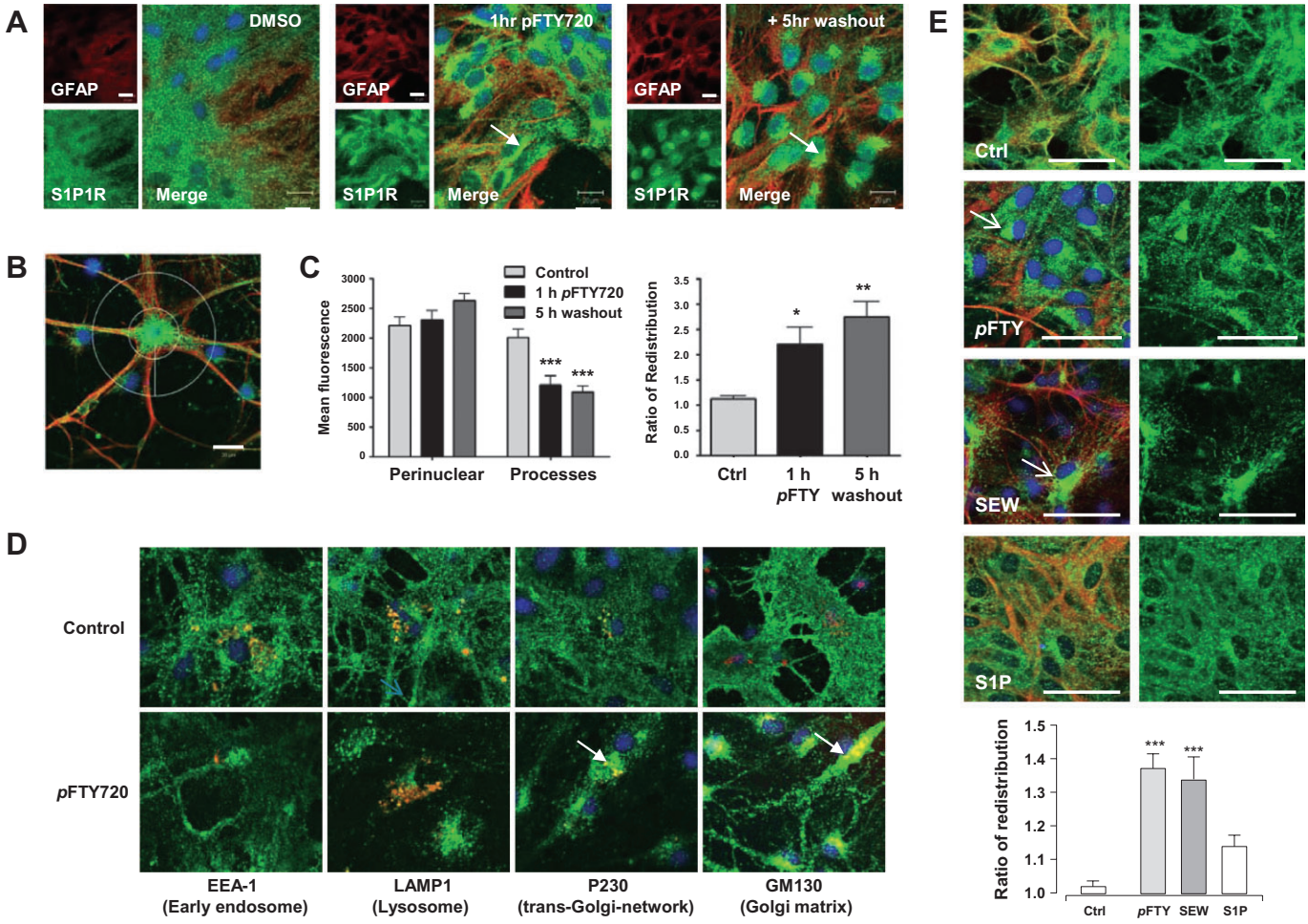

Figure 2

pFTY720 induced long lasting redistribution of S1P1R to the trans-Golgi-network in astrocytes. (A) DMSO (vehicle control), 1 μM *p*FTY720 treatment for 1 h (positive control) and 1 μM *p*FTY720 treatment for 1 h followed by a 5-h washout period. Scale bars 20 μm. (B) Calculation of S1P1R redistribution was performed by taking mean fluorescent measurements from the 'perinuclear zone' defined as S1P1R staining <10 μm from the nucleus (inner circle) and the 'process zone' defined as S1P1R staining >35 μm from the nucleus (outer circle). (C) Bar graphs show changes in the levels of perinuclear and cytoplasmic S1P1R staining in astrocytes treated with *p*FTY720. Statistical analysis shows the level of redistribution and also the ratio of nuclear : cytoplasmic S1P1R expression (***$P < 0.001$ vs. control, two-way ANOVA and Bonferroni *post hoc* test). (D) Vehicle control and *p*FTY720 treated astrocytes were stained with organelle marker antibodies (red) including early endosome (EEA-1), trans-Golgi-network (p230), lysosome (LAMP1) and Golgi matrix (GM130). S1P1R staining overlapped with p230 and GM130 markers indicative of localization of the redistributed S1P1R to the TGN and Golgi matrix. (E) S1P1R redistribution was investigated following treatment with DMSO (Ctrl), *p*FTY720 (1 μM, 1 h), the selective S1P1 agonist SEW2871 (1 μM, 1 h) and the endogenous ligand S1P (1 μM, 1 h). Scale bars 50 μm. Bar graph shows statistical analysis of redistribution (***$P < 0.001$ vs. control, one-way ANOVA and Bonferroni *post hoc* test). Unless indicated, cells were immunostained with GFAP Ab (red) and S1P1R Ab (green), cell nuclei appear as blue (Hoescht) and arrows indicate areas of S1P1R redistribution as determined by perinuclear staining.

and GFAP and the MNP301 peptide visualized in green (Figure 3C). This data further confirmed cell transduction by MNP301 after a brief (2 h) exposure. Notably, visualization of the FITC-based fluorescence 2 days post-transduction may reflect stability of the FITC label, rather than long-term cellular stability of the peptide, *per se*. Following validation that MNP301 transduces astrocytes, its effects on *p*FTY720-induced redistribution of S1P1R were investigated. Rat astrocyte cultures were transduced with a non-FITC labelled, Tat-fused version of MNP301 (100 μg·mL^{-1}) for 1 h at 37°C and cells were then washed three times in serum-free media to remove MNP301 and subsequently treated with or without *p*FTY720 (1 μM) for 1 h at 37°C. The data showed that pre-incubation of astrocytes with 100 μg·mL^{-1} MNP301 attenuated *p*FTY720-mediated redistribution of S1P1R (Figure 3D). Cumulative frequency curves, generated by automated image analysis, for each treatment group displayed a marked increase in the relative frequency of cells exhibiting a ratio of redistribution of greater than 1 for cells treated with *p*FTY720, while pre-incubation with MNP301 attenuated this distribution shift (Figure 3E). In addition, manual image analysis confirmed qualitative assessment showing that pre-incubation with MNP301 significantly attenuated *p*FTY720-induced redistribution of S1P1R (Figure 3F).

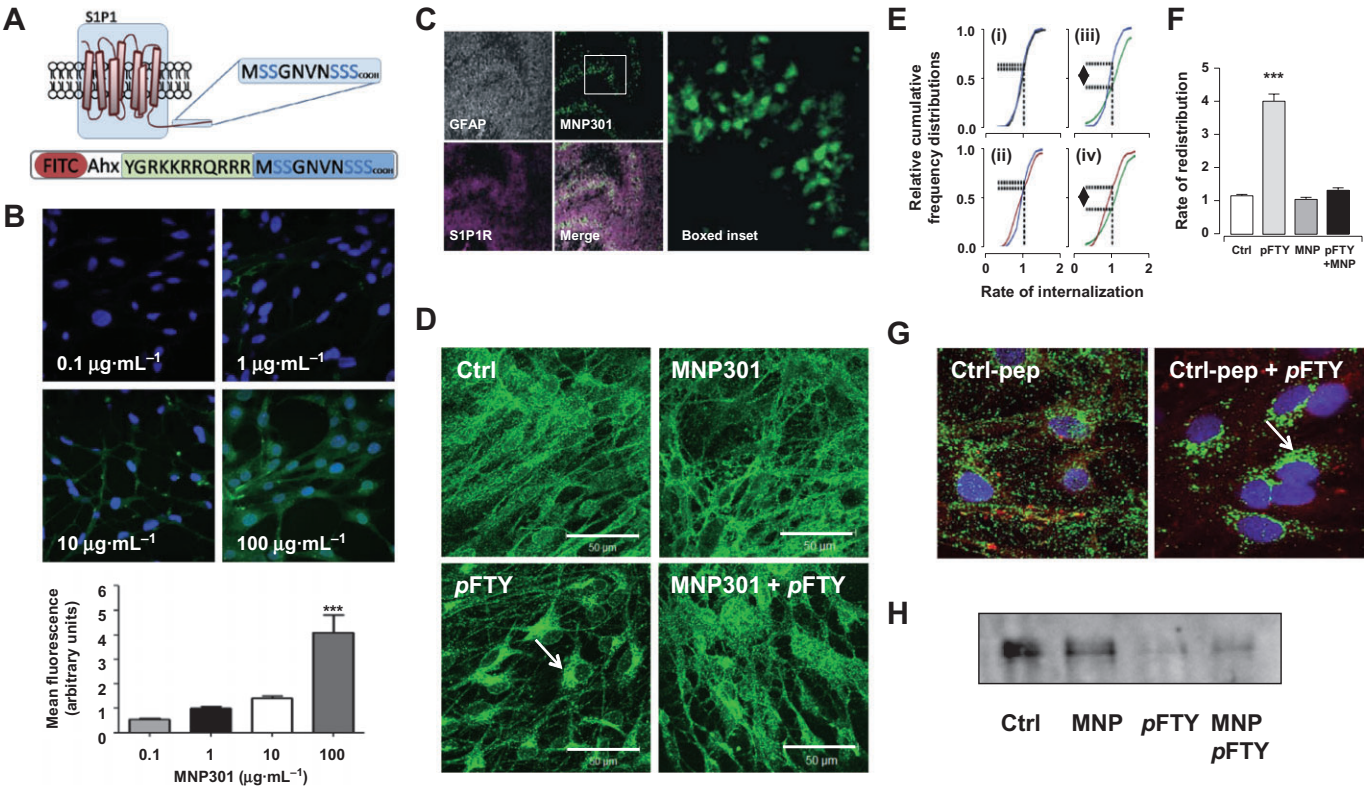

Figure 3

MNP301 prevents pFTY720-induced redistribution of S1P1R. (A) The structure of MNP301 is shown and is composed of a FITC tag, a cell transduction Tat sequence and the last 10 residues of ct-S1PR (FITC-Ahx-YGRKKRRQRRR-MSSGNVNSSS). (B) Pure astrocytes cultures were treated with increasing concentrations of FITC-Tat-MNP301 for 1 h at 37°C and direct FITC fluorescence (green) was observed at a wavelength of 488 nm by confocal microscopy. Graph shows mean fluorescence calculated from five images per condition. Significant cellular transduction was observed following incubation of astrocytes with 100 μg·mL^{-1} MNP301 (***P < 0.001 vs. control, one-way ANOVA and Bonferroni *post hoc* test). (C) Organotypic cerebellar culture were treated for 2 h with FITC-Tat-MNP301 (250 μg·mL^{-1}) and placed in fresh medium for 2 days. Slices were stained for S1P1R Ab (purple) and GFAP Ab (grey) 2 days post-tansduction with MNP301 (green). Boxed inset shows magnification of white box of FITC-Tat-MNP301 fluorescence. (D) Astrocytes were treated with *p*FTY720 (1 μM) for 1 h at 37°C in the presence and absence of a non-FITC labelled, Tat-fused MNP301 (100 μg·mL^{-1}). Scale bars 50 μm. (E) Relative cumulative frequency distribution curves, as determined by automated image analysis, display a marked increase (>20% of total cells analysed) in the number of astrocytes exhibiting S1P1R redistribution in the *p*FTY720-treated group; as measured by the ratio of perinuclear : cytoplasmic fluorescence. Co-treatment with MNP301 attenuated this rightward distribution shift. The figures show no difference in S1P1R redistribution between (i) control vs. MNP301 or (ii) MNP301 vs. MNP301 + *p*FTY720, and a difference of S1P1R redistribution between (iii) *p*FTY720 vs. MNP301 and (iv) *p*FTY720 vs. MNP301 + *p*FTY720. The number of cells analysed per treatment group were vehicle control = 154; MNP301 = 144; *p*FTY720 = 225; MNP301 + *p*FTY720 = 264. (F) Statistical analysis of S1P1R redistribution, as derived from manual image analysis, indicates that MNP301 significantly inhibited *p*FTY720 induced redistribution to the TGN. Data expressed as mean ± SEM of three separate experiments (***P < 0.001 vs. *p*FTY720 alone, one-way ANOVA, Bonferroni *post hoc* test). (G) Treatment of rat astrocytes for 1 h at 37°C with 100 μg·mL^{-1} control peptide (non-FITC labelled, Tat-fused Ctrl-pep; YGRKKRRQRRR-VCMGDHWFDV) did not alter S1P1R localization in the presence or absence of *p*FTY720 (1 μM for 1 h at 37°C). Unless indicated, cells were immunostained with GFAP Ab (red) and S1P1R Ab (green), cell nuclei appear as blue (Hoescht) and arrows indicate areas of redistribution as determined by perinuclear staining. (H) Human astrocytes were pretreated with or without MNP301 (100 μg·mL^{-1} for 1 h) followed by treatment with or without pFTY720 (1 μM for 1 h). Astrocytes were then incubated with non-permeable biotin (0.5 mg·mL^{-1} for 30 min). The cell surface biotin proteins were immunoprecipitated using streptavidin-coated agarose beads and levels of cell surface biotinylated S1P1R were measured by Western blotting. Data shown is a representative of three independent experiments.

Notably, a tat-fused unrelated control peptide sequence (YGRKKRRQRRR-VCMGDHWFDV) had no effect on *p*FTY720-mediated redistribution of S1P1R, confirming no effects of the tat sequence on S1P1R trafficking (Figure 3G). A FITC-labelled version of this control peptide was confirmed to transduce astrocytes in a dose-dependent manner similar to MNP301 (data not shown). In addition to these immunocytochemistry experiments, cell surface biotinylation studies were also performed to demonstrate the effects of pFTY720 on S1P1R surface expression in the presence and absence of MNP301. The data showed pFTY720 reduced S1P1R surface expression in astrocytes, while MNP301 pretreatment attenuated the effects of pFTY720 (Figure 3H). Taken together, this data showed that MNP301, a peptide modelled on the last 10 amino acids of the S1P1R, prevented *p*FTY720-induced redistribution of S1P1R.

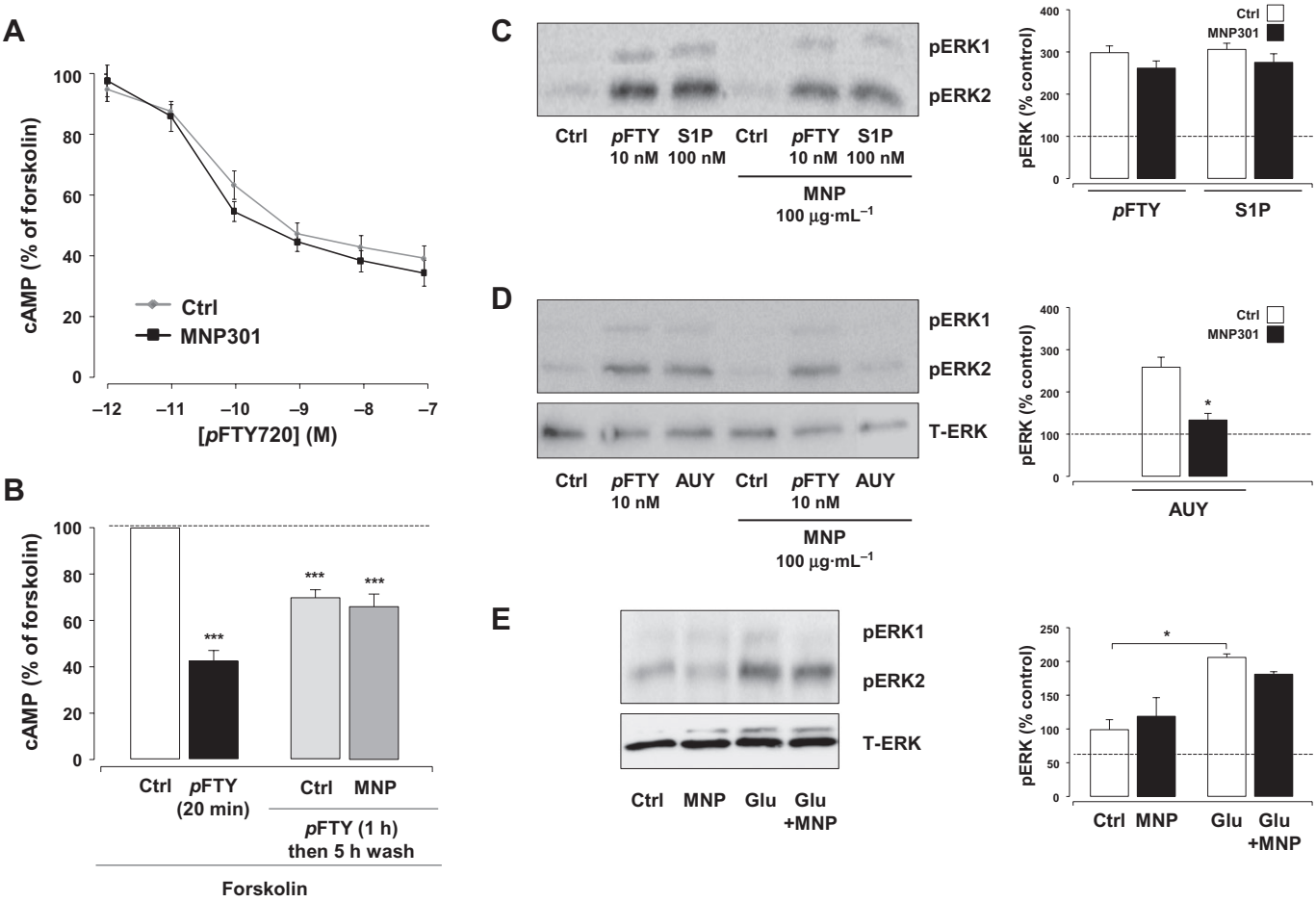

Figure 4

Continued pFTY720-induced cAMP signalling of S1P1R in astrocytes. (A) Shown are the concentration-response curves of acute *p*FTY720 (1 µM for 20 min) treatment inhibiting forskolin-induced cAMP levels in astrocytes pretreated with or without MNP301 (±100 µg·mL^{-1} for 1 h). Data presented as percentage cAMP inhibition and is representative of three separate experiments. (B) The acute effect of *p*FTY720 (1 µM for 20 min) on forskolin-induced cAMP formation in astrocytes is shown (lane 2). The percentage of cAMP inhibition in astrocytes pre-incubated without (lane 3) or with (lane 4) MNP301 (100 µg·mL^{-1} for 1 h) followed by addition of *p*FTY720 (1 µM for 1 h) then washed and cAMP levels measured 5 h later is shown. Data are representative of five independent experiments. (***$P < 0.001$ vs. control, one-way ANOVA, Bonferroni *post hoc* test). (C) Treatment of purified rat astrocyte cultures with pFTY720 (10 nM for 10 min) and S1P (100 nM for 10 min) induced a significant increase in the phosphorylation of ERK (pERK) as determined by Western blotting. Pretreatment with MNP301 (100 µg·mL^{-1} for 1 h) did not significantly reduce the levels of pERK. (D) AUY954 (10 nM for 10 min) induced a significant increase in pERK in astrocytes that was significantly inhibited by pretreatment MNP301 (100 µg·mL^{-1} for 1 h) (*$P < 0.05$, one-way ANOVA with Neumann–Keuls *post hoc* test). (E) The significant increase in levels of pERK induced by glutamate (600 µM for 10 min) (*$P < 0.05$ based on one-way ANOVA and Bonferroni *post hoc* analysis) were not significantly altered by MNP301 pretreatment (100 µg·mL^{-1} for 1 h). (D-E) Data expressed as mean ± SEM of two–four separate experiments. The levels of phosphorylated ERK (P-ERK) were expressed as arbitrary units of optical density, following the correction for content of total ERK (T-ERK).

*p*FTY720-induced continued cAMP signalling can be uncoupled from redistribution of S1P1R

Previous studies, using HUVECs showed that treatment with *p*FTY720 followed by a 5-h washout period induced a continued inhibition of cAMP production (Mullershausen *et al.*, 2009). Therefore, the ability of a *p*FTY720-redistributed pool of S1P1R in astrocytes to inhibit forskolin-induced cAMP formation after washout of the drug was determined. In the first set of experiments, the effect of MNP301 on *p*FTY720-mediated acute signalling of S1P1Rs was examined. Increasing concentrations of *p*FTY720 (20 min treatment) generated IC_{50} values for forskolin-induced cAMP formation of 0.07 ± 0.24 nM and 0.05 ± 0.14 nM with and without pretreatment of MNP301 (100 µg·mL^{-1} for 1 h), respectively (Figure 4A). In the second set of experiments, the effect of MNP301 on *p*FTY720-mediated continued inhibition of cAMP levels was examined. The data showed that *p*FTY720 (1 µM for 20 min) attenuated forskolin-induced cAMP formation (42.1% ± 4.8% inhibition) (Figure 4B, lane 2) compared to forskolin alone (Figure 4B, lane 1). In agreement with previous findings using HUVECs (Mullershausen *et al.*, 2009), forskolin-induced cAMP formation remained markedly attenuated in astrocytes treated with *p*FTY720 (1 µM for 1 h) even 5 h after washout of the drug (69.7% ± 5.2% inhibition) (Figure 4B, lane 3),

thus providing evidence for continued cAMP signalling. To examine the role of *p*FTY720-induced redistribution of S1P1R, its effects on forskolin-induced cAMP formation were determined in the presence of MNP301. The data showed that despite attenuation of S1P1R redistribution by *p*FTY720 (Figure 3), the continued cAMP inhibition caused by *p*FTY720 treatment (1 μM for 1 h followed by 5 h washout) was not altered by pretreatment of MNP301 (100 μg·mL^{-1} for 1 h) (65.7% ± 3.3% inhibition) (Figure 4B, lane 4). Collectively, the data suggests that while MNP301 prevents *p*FTY720-induced redistibution of S1P1Rs, this peptide does not affect cAMP signalling of these receptors. This data also refines a previous hypothesis that *p*FTY720 induces continued cAMP inhibition via internalized S1P1R (Mullershausen *et al.*, 2009) and suggests that redistibution of S1P1R caused by *p*FTY720 can be uncoupled from continued cAMP signalling.

MNP301 prevents pERK-signalling induced by the selective S1P1R compound AUY954

An alternative explanation for the observed effects of pFTY720-mediated continued signalling on cAMP levels in astrocytes may due to activation of other S1PRs. However, supporting the specific role of the S1P1R subtype in continued cAMP signalling are the following previous findings (i) at the concentration used in the current studies, pFTY720 is not known to bind S1P2R, (ii) compared to the S1P1R selective compounds AUY954 or SEW2871, the effects of pFTY720 on cAMP levels do not significantly differ in astrocytes (Mullershausen *et al.*, 2007) and (iii) the other major S1PR expressed in rat astrocytes appears to be S1P3R (Mullershausen *et al.*, 2007), however pFTY720 does not induce persistent S1P3R signalling (Mullershausen *et al.*, 2009). In addition to these reports, the specific role of S1P1Rs and the specificity of MNP301 inhibiting the S1P1R subtype, but not other S1PRs, was further investigated. To do this, the effect of MNP301 on S1PR-mediated pERK signalling was examined. The data showed that S1P (304 ± 12%) and pFTY720 (296 ± 14%) induced an increase in the levels of pERK in a similar manner under control versus MNP301 pretreatment conditions (Figure 4C). In contrast, MNP301 significantly blocked AUY954-mediated induction of pERK down to control levels (255 ± 25% vs. 130 ± 25%) (Figure 4D). Importantly, MNP301 did not alter glutamate induced increase in the levels of pERK showing selectivity toward S1P receptors (Figure 4E). Taken together, these data showed that MNP301 prevented pERK signalling induced by selective S1P1R compounds (such as AUY954), but not by pan-S1P1R compounds (such as S1P or pFTY720) or other receptors coupled to pERK (such as glutamate receptors). These results support the suggestion that MNP301 is a specific S1P1R modulator and not a pan-S1PR modulator or modulator of pERK-signalling *per se*. Moreover while MNP301 prevents pFTY720-induced redistibution of S1P1Rs and S1P1R-mediated pERK-signalling, it does not alter cAMP-signalling or cAMP-continued signalling, suggesting pathway specific modulatory effects of this peptide.

Functional antagonism of S1P1R-mediated Ca^{2+} signalling in astrocytes

It has been shown previously that S1PRs in astrocytes respond to agonist activation in a Ca^{2+}-dependent manner (Mullershausen *et al.*, 2007). To further investigate S1PR signalling events in astrocytes, the ability of both S1P (Figure 5A) and the S1P1R selective compound AUY954 (Figure 5B) to elicit Ca^{2+} signals was examined. Astrocytes were starved for 3 h in serum-free media prior to stimulation with increasing concentrations of both S1P and AUY954. Changes in Ca^{2+} levels were recorded over a time course of 240 s; following addition of test compound for 150 s and glutamate was added for a further 60 s. Treatment with both the pan-S1PR agonist S1P and the S1P1R selective compound AUY954 caused concentration dependent increases in Ca^{2+} levels in primary rat astrocytes (Figure 5). The data confirmed S1P1Rs modulate Ca^{2+} signalling in astrocytes. Given that S1P1Rs are coupled exclusively to G_i, the results also suggest that S1P1R mediated Ca^{2+} signalling (induced by the S1P1R selective compound AUY954) occurs via $G_{\beta\gamma}$ subunit activation (Birnbaumer, 1992). To examine the effect of S1P1R redistribution on Ca^{2+} signalling, primary rat astrocytes were pretreated with various S1PR ligands. Serum starved cells were pretreated with 1 μM S1P, pFTY720 and AUY954 for 1 h followed by a 3-h washout period to ensure Ca^{2+} levels had returned to baseline prior to restimulation with 1 μM S1P (Figure 6A). The data showed that, compared to control, pretreatment with 1 μM S1P, pFTY720 or AUY954 significantly reduced the ability of astrocytes to respond to further stimulation by S1P ($P < 0.001$ pretreatment vs. control, as determined by unpaired *t*-test). Given that S1P does not evoke long lasting redistribution of S1P1Rs (Figure 2E), this attenuation of Ca^{2+} signalling is unlikely due to altered S1P1R cellular localization and possibly caused by uncoupling of the receptor from the Ca^{2+} signalling pathway, or due to a conformational change of S1PRs induced by S1P, pFTY720 and AUY954 pretreatments. Notably, the attenuated Ca^{2+} signalling is unlikely due to the depletion of Ca^{2+} stores *per se*, as the cells responded to subsequent application of glutamate (30 μM) (Figure 6). One of the confounding factors in these experiments is the pan-S1PR properties of S1P and possible effects of S1P on other S1PRs (especially S1P3Rs) expressed in astrocytes (Mullershausen *et al.*, 2007). Thus, to specifically evaluate S1P1R-mediated Ca^{2+} signalling, primary rat astrocytes were pretreated with 1 μM S1P, pFTY720 and AUY954 for 1 h, followed by a 3-h washout period before restimulating with the specific S1P1R ligand AUY954 (1 μM) (Figure 6B). In agreement that pretreatment with S1P, pFTY720 or AUY954 causes a long lasting antagonism of Ca^{2+} signalling, the data showed that pretreatment with these three compounds significantly attenuated astrocyte response to restimulation with AUY954 ($P < 0.001$ pretreatment vs. control, as determined by unpaired *t*-test) (Figure 6B). Of note, pretreatment with S1P, pFTY720 or AUY954 partially reduced the effects of S1P restimulation on Ca^{2+} levels (Figure 6A), while these pretreatments completely abrogated the Ca^{2+} response to AUY954 restimulation (Figure 6B). Given the predominate expression of S1P1R and S1P3R in astrocytes, these results can be best explained by suggesting that S1P regulates Ca^{2+} signalling in astrocytes via S1P1R, S1P3R (and possibly S1P2,5R), *p*FTY720 by S1P1R, partially by S1P3R (and possibly S1P5R), and AUY954 specifically by S1P1R. These results would also suggest that the S1P1R subtype contributes to approximately 50% of the observed Ca^{2+} response to S1P stimulation, which is sensitive to prestimulation with

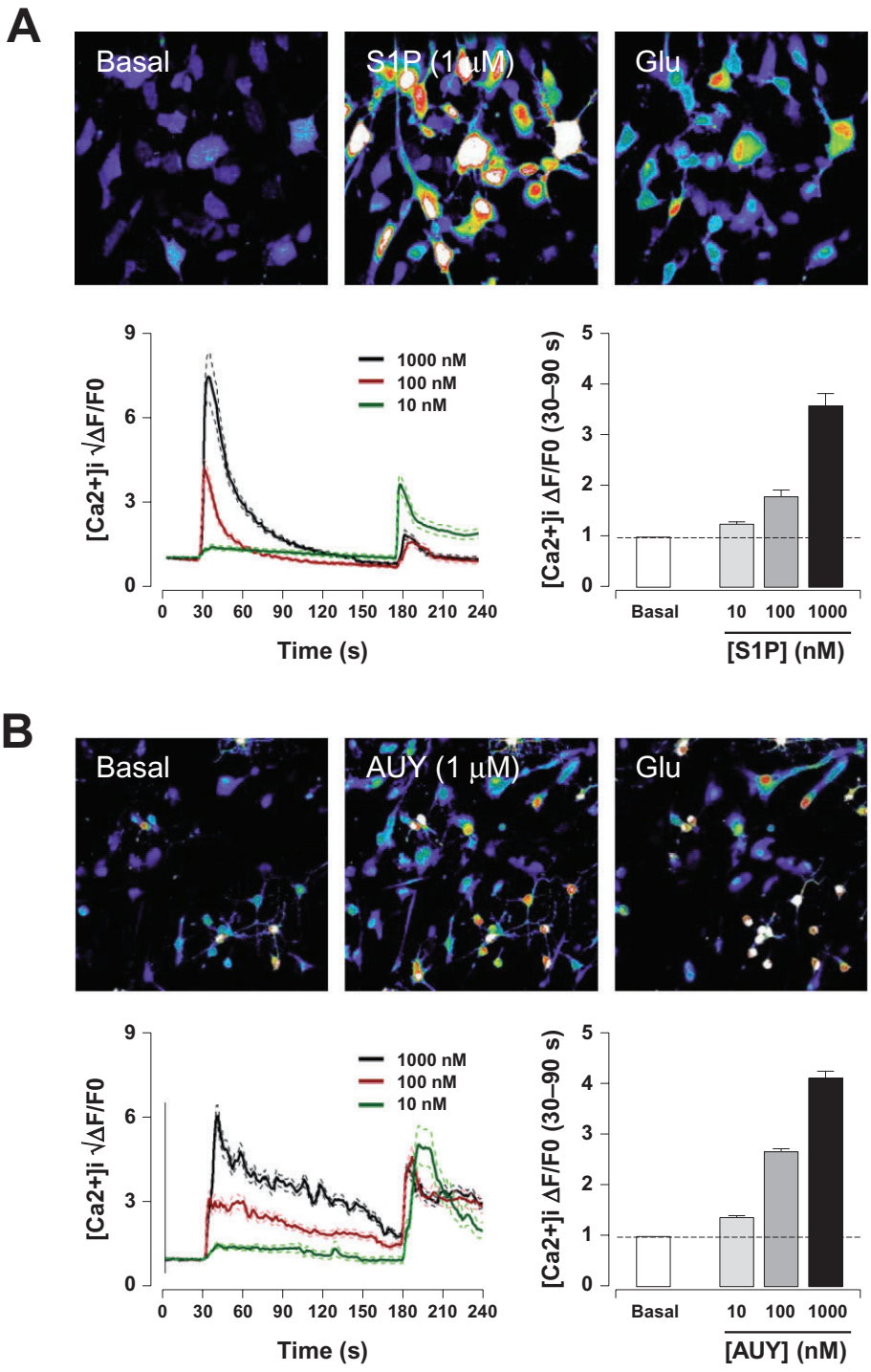

Figure 5

S1PR agonists induce a concentration dependent increase in Ca^{2+} levels in primary rat astrocytes. Increasing concentrations of (A) the natural ligand S1P and (B) the S1P1 specific agonist AUY954 induce a concentration dependent increase in Ca^{2+} levels. Representative images show time-lapse series, at basal levels time point 0 s (basal), after addition of 1 μM S1P or AUY954 at 30 s (S1P or AUY), and after stimulation with 30 μM glutamate at 180 s (Glu). Traces depict changes in Ca^{2+} levels over time. Bar graphs (30–90 s) show that S1P and AUY954 cause a concentration dependent increase in Ca^{2+} levels. Data represented as mean ± SEM. Cells counted, S1P 1 μM = 200, S1P 100 nM = 185, S1P 10 nM = 132; AUY 1 μM = 235, AUY 100 nM = 171, AUY 10 nM = 85.

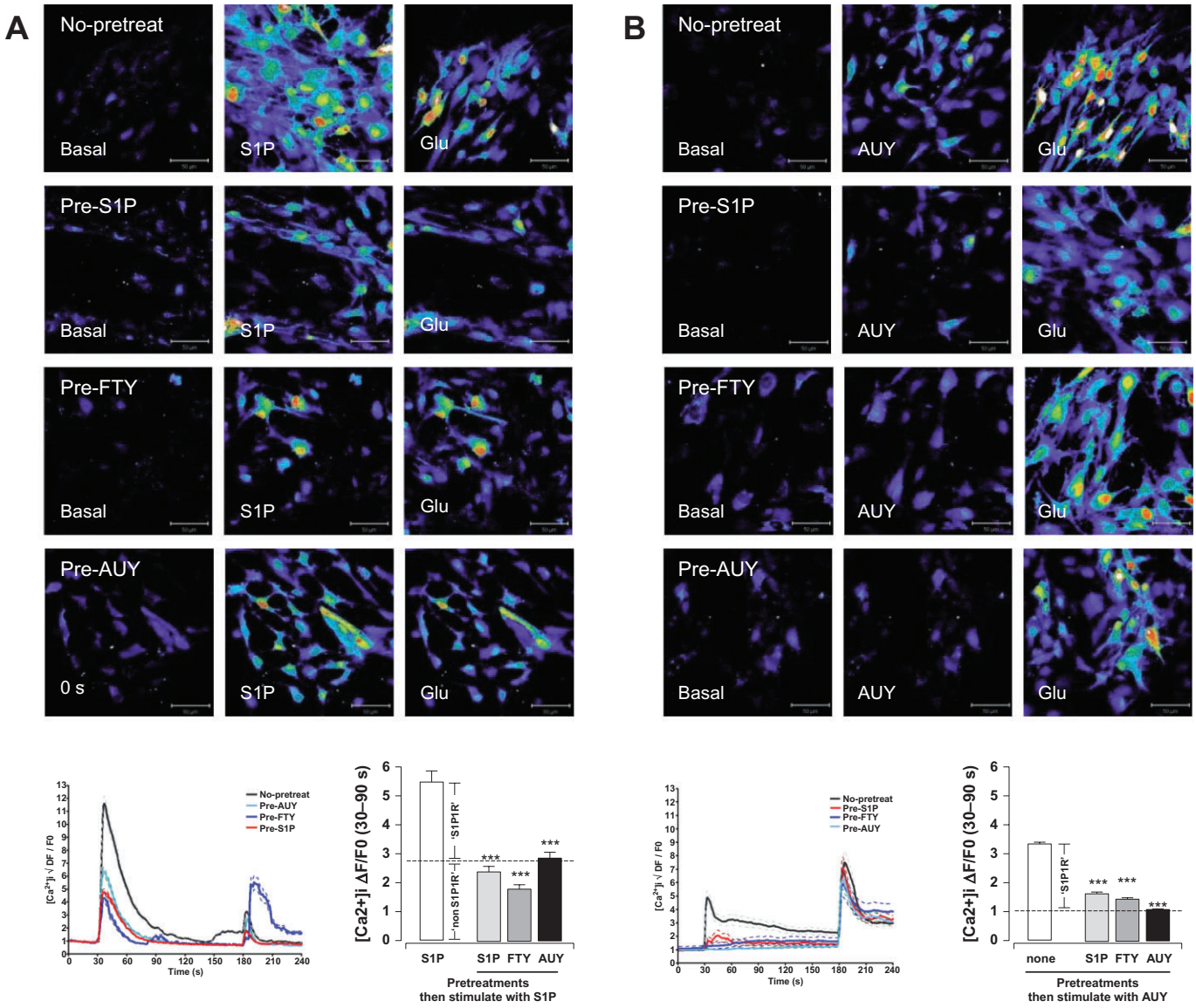

Figure 6

S1PR pre-activation inhibits further S1PR mediated increases in Ca^{2+} levels in astrocytes. Pre-treatment with S1P, pFTY720 and AUY954 significantly inhibited changes in Ca^{2+} levels in response to a secondary treatment with (A) S1P or (B) AUY954. Representative images show time-lapse series, before addition of S1P or AUY954 (0 s, basal), after addition of 1 μM S1P or AUY954 (30 s) and after stimulation with 30 μM glutamate at 180 s (Glu). Traces depict changes in Ca^{2+} levels over time. Bar graphs (30–90 s) show data represented as mean ± SEM, with a total of eight observations for all conditions (***$P < 0.001$ pretreatment vs. control, as determined by unpaired *t*-test).

S1P, pFTY720 or AUY954. In contrast, approximately 50% of the observed Ca^{2+} response to S1P stimulation is likely via an S1P3R (and possibly S1P2,5R) evoked response that is not sensitive to prestimulation with S1P, pFTY720 or AUY954. From this data, it appears that S1PR ligands can differentially regulate cAMP (Figure 4), pERK (Figure 4) and Ca^{2+} signalling pathways (Figure 6) and that continued S1P1R signalling or functional antagonism can be independent from receptor redistribution. This data also suggests that, similar to *p*FTY720, functional antagonism can be caused by the natural ligand S1P in specific pathways such as Ca^{2+} signalling.

MNP301 antagonizes S1P1R mediated increases in Ca^{2+} levels in astrocytes

Having shown that MNP301 prevented *p*FTY720 induced redistribution of S1P1R (Figure 3), blocked specific S1P1R-mediated pERK signalling (Figure 4), without altering the continued effects of *p*FTY720 on cAMP signalling (Figure 4), its effect on S1P1R-mediated Ca^{2+} signalling was examined. Primary rat astrocytes were incubated with 100 $\mu g \cdot mL^{-1}$ concentration of MNP301 for 1 h followed by a 3-h wash-out period. Cells were then stimulated with 1 μM S1P (Figure 7A,C) and 1 μM AUY954 (Figure 7B,D). Statistical

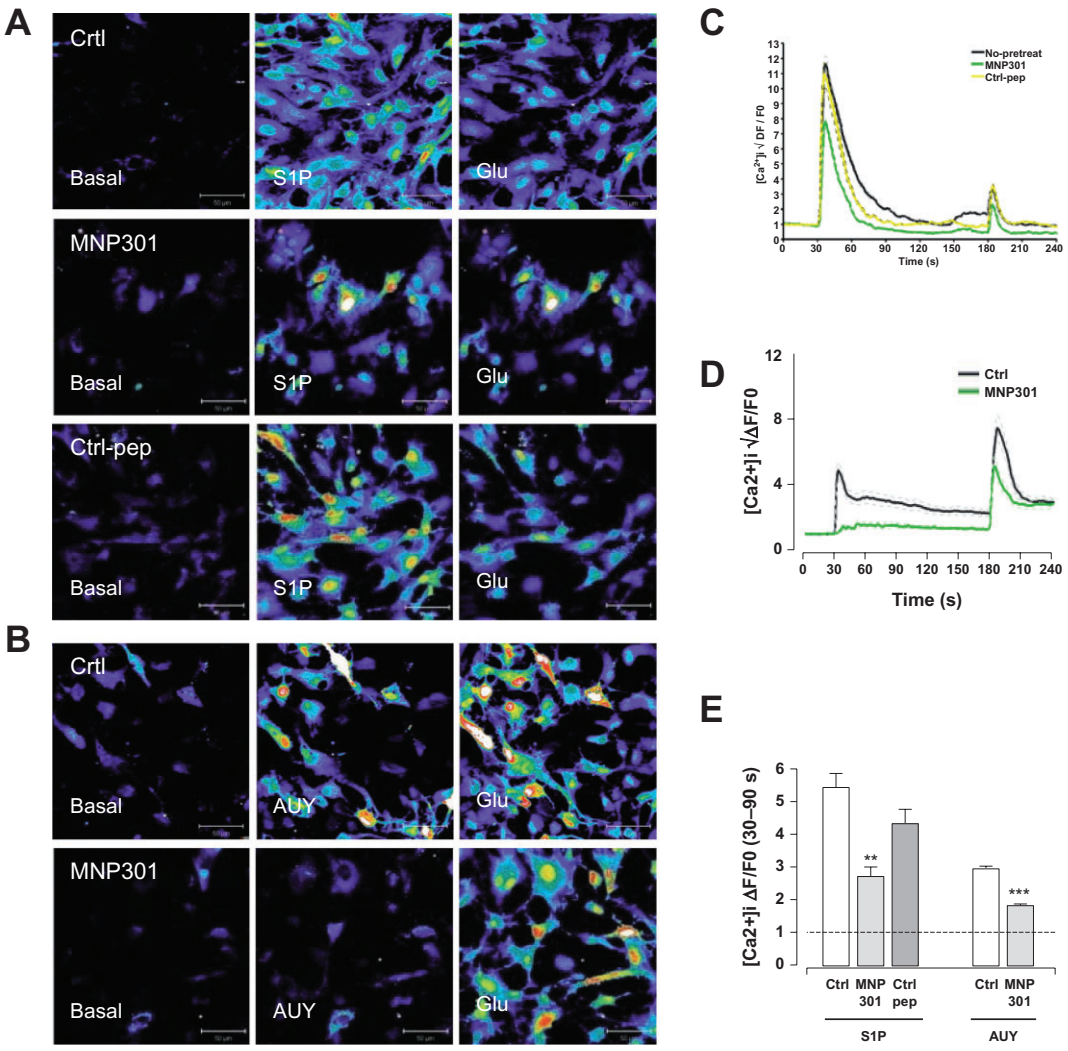

Figure 7

MNP301 antagonizes S1P1 receptor mediated increases in Ca^{2+} levels in astrocytes. Pretreatment with 100 μg·mL^{-1} MNP301, but not the unrelated control peptide (Ctrl-pep), significantly inhibited changes in Ca^{2+} levels in response to a secondary treatment with (A) S1P or (B) AUY954. Representative images show time-lapse series, before addition of S1P or AUY954 (0 s, basal), after addition of 1 μM S1P or AUY954 (30 s) and after stimulation with 30 μM glutamate at 180 s (Glu). Traces depict changes in Ca^{2+} levels over time induced by (C) S1P and (D) AUY954. (E) Bar graph show data (30–90 s) represented as mean ± SEM (**$P < 0.01$ pretreatment vs. control, as determined one-way ANOVA). Cells counted, Ctrl-S1P = 648, MNP301-S1P = 612; Ctrl-AUY = 479, MNP301-AUY = 399.

analysis showed that MNP301 significantly reduced S1P and attenuated AUY954 (Figure 7E) induced increase in Ca^{2+} levels in astrocytes ($P < 0.01$ pretreatment vs. control, as determined one-way ANOVA). In contrast the unrelated peptide had no effect on S1P-induced Ca^{2+} signalling in rat astrocytes (as determined by one-way ANOVA), indicating that the effects of MNP301 on S1P1R-induced Ca^{2+} signalling is sequence specific and not due to the TAT epitope (Figure 7A,C,E). The differential level of inhibition by MNP301 on S1P- and AUY954-mediated Ca^{2+} signalling is also in agreement with a selective effect of MNP301 on the S1P1R subtype. This antagonistic effect of MNP301 may be due to interference of interactions between adaptor proteins that ensure correct S1P1R conformation and/or regulation of second messenger proteins necessary for the propagation of Ca^{2+} signals at the extreme ct-S1P1R.

Human astrocytes display S1PR-mediated increase in Ca^{2+} from a predominantly extracellular source

It has been shown previously that S1PR evoked Ca^{2+} signalling in astrocytes is due to activation of both intracellular stores and entry of extracellular Ca^{2+} into the cell (Giussani *et al.*, 2007). However, the source of Ca^{2+} in response to specific activation of S1P1R subtype remains unclear. To evaluate this, the effect of both antagonists of IP3/ryanodine receptors (dantrolene) and chelators of extracellular Ca^{2+} (EGTA) on S1PR-induced elevations of Ca^{2+} were examined. These studies were performed using human astrocytes, which were confirmed to express endogenous S1PRs (Figure 8A). The effect of both S1P and the S1P1R specific compound SEW2871 on Ca^{2+} levels in human astrocytes was demon-

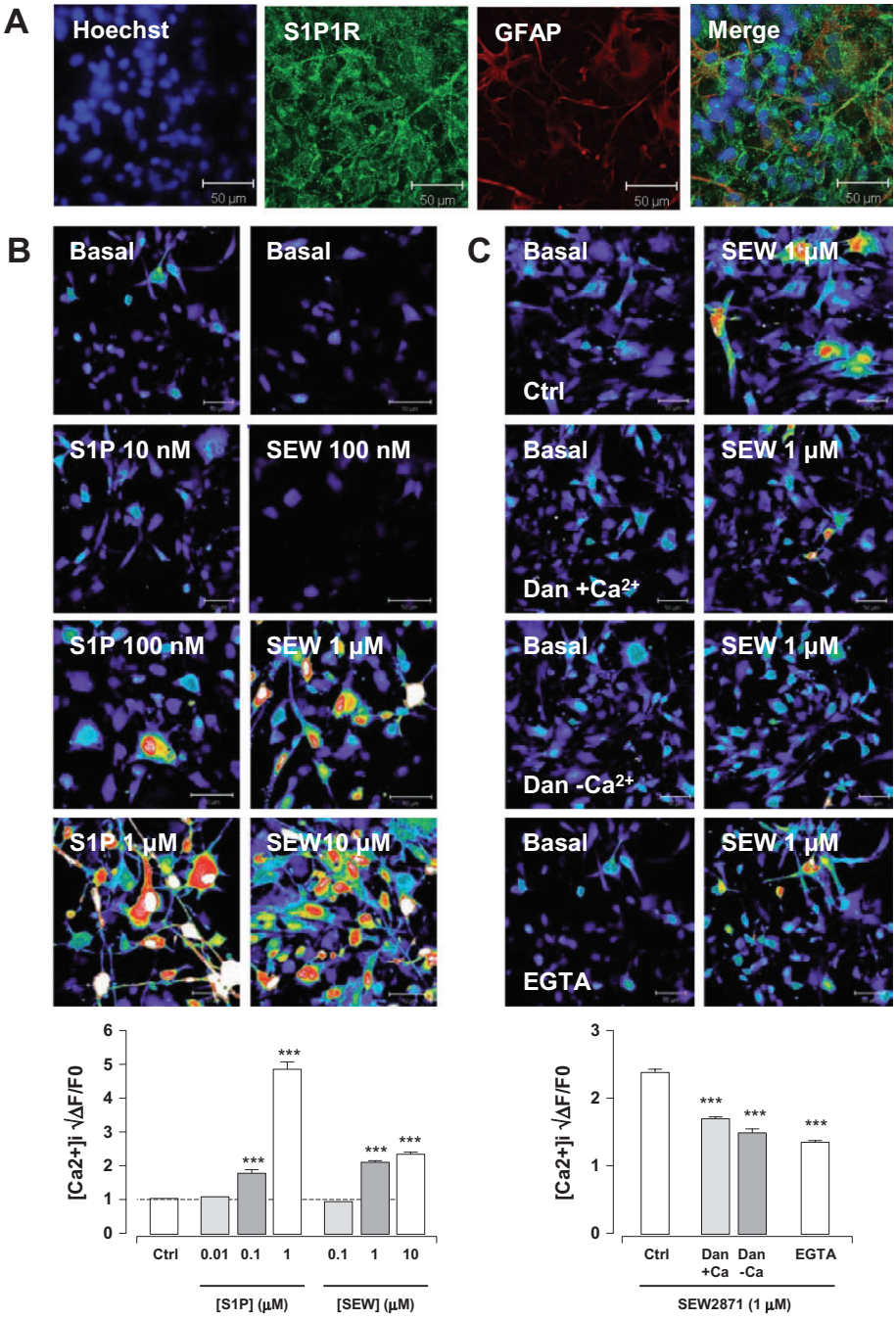

Figure 8

Agonism of S1PRs evokes increases in Ca^{2+} levels in human astrocytes from a predominantly extracellular source. (A) Human astrocyte cultures stained for GFAP (red) and S1P1R (green), show expression of S1P1 receptors in astrocytes. (B) Both S1P and the S1P1 specific compound SEW2871 induced a concentration dependent increase in Ca^{2+} levels in human astrocytes. Representative images show time-lapse series, after addition of increasing concentrations of S1P and SEW2871 (30 s). (C) Pretreatment of human astrocytes with 30 µM dantrolene (Dan), in the presence and absence of Ca^{2+} significantly reduced cells response to 1 µM SEW2871 (***$P < 0.001$ dantrolene vs. SEW2871 one-way ANOVA, Dunnetts *post hoc* test). Pretreatment with 1 mM EGTA significantly inhibited 1 µM SEW2871 induced increases in Ca^{2+} levels (***$P < 0.001$ EGTA vs. SEW2871, unpaired *t*-test). Bar graphs (30–90 s) show averaged data ± SEM, $n = 3$ (***$P < 0.001$ vs. control, one-way ANOVA and Bonferroni *post hoc* test). Scale bars 50 µm.

strated. Data showed that both S1P and SEW2871 ($P < 0.001$, 1 µM and 10 µM vs. control, one-way ANOVA and Bonferroni *post hoc* test) induced a concentration dependent increase in Ca^{2+} levels in human astrocytes (Figure 8B). S1P induced higher levels of Ca^{2+}, likely due to activation of S1P1R and S1P3R (and possibly other S1PRs), versus the selective activation of S1P1Rs by SEW2871. Human astrocytes were pretreated with 30 µM dantrolene for 10 min and subsequently

stimulated with 1 μM SEW2871 in both Ca^{2+} containing HBSS and HBSS minus Ca^{2+}. Cells pretreated with 30 μM dantrolene (+Ca^{2+}) showed a slow increase in Ca^{2+} levels, peaking at 90 s post SEW2871 stimulation (Figure 8C). In contrast, cells pretreated with 30 μM dantrolene (-Ca^{2+}) showed a relatively slower Ca^{2+} signalling, with cells only beginning to respond ~80 s post SEW2871 stimulation (Figure 8C). Both dantrolene treatments, while not completely inhibiting elevations in Ca^{2+} levels, significantly reduced S1P1R mediated Ca^{2+} responses ($P < 0.001$, dantrolene (+Ca^{2+}) and dantrolene (–Ca^{2+}) vs. control, one-way ANOVA and Bonferroni *post hoc* test). To examine the contribution of extracellular sourced Ca^{2+} in S1P1R evoked Ca^{2+} signalling, human astrocytes were pretreated with 1 mM EGTA for 10 min followed by stimulation with SEW2871 dissolved in HBSS minus Ca^{2+}. Data showed that cells showed a significantly reduced response to SEW2871 stimulation in the presence of the extracellular chelating agent EGTA ($P < 0.001$, EGTA vs. control, one-way ANOVA and Bonferroni *post hoc* test) (Figure 8C). Taken together, this data demonstrated S1P1R evoked Ca^{2+} signalling utilizes predominantly Ca^{2+} from an extracellular source.

Discussion

Previous studies have reported that modulation of S1P1Rs by *p*FTY720 regulates several intracellular signalling pathways in rat astrocytes, including the inhibition of adenylyl cyclase, activation of phospholipase C, increase of ERK phosphorylation and rise of intracellular Ca^{2+} levels (Mullershausen *et al.*, 2007; Osinde *et al.*, 2007). It has also been demonstrated that S1P1R activation promotes astrocyte migration (Mullershausen *et al.*, 2007) in line with S1P-induced migration of neural stem cells and oligodendrocyte precursors (Kimura *et al.*, 2007; Novgorodov *et al.*, 2007). Evidence suggests a specific role for the S1P1R subtype in astrocytes, as the effects of *p*FTY720 and S1P are mimicked by selective S1P1R agonists and blocked by S1P1R antagonists (Mullershausen *et al.*, 2007; Osinde *et al.*, 2007). More recently, the specific knockdown of S1P1Rs in astrocytes has been shown to limit the effects of *p*FTY720 in EAE providing strong support for a key role of this receptor subtype in astrocyte function (Choi *et al.*, 2011).

In the current study, using rat astrocyte cultures, the data showed that treatment with *p*FTY720 or the S1P1R-selective agonist SEW2871, but not S1P, caused redistribution of S1P1Rs towards the trans-Golgi-network in a concentration- and time-dependent manner, similar to that found in CHO cells stably expressing S1P1R and HUVECs expressing endogenous S1P1R (Mullershausen *et al.*, 2009). These S1P1Rs displayed long lasting redistribution, remaining inside the cell for at least 5 h after washout of *p*FTY720. To investigate whether *p*FTY720-induced transient agonism and redistribution of S1P1Rs caused subsequent functional antagonism (Brinkmann *et al.*, 2002; Goetzl and Graler, 2004) or continued signalling (Mullershausen *et al.*, 2009) of S1P1Rs, both cAMP and Ca^{2+} signalling was measured in rat astrocytes. Similar to HUVECs (Mullershausen *et al.*, 2009), rat astrocytes treated with *p*FTY720 exhibited continued cAMP signalling as shown by long lasting inhibition of forskolin-induced cAMP formation. In contrast, treatment of rat astrocytes with *p*FTY720 caused transient Ca^{2+} signalling and subsequent functional antagonism. The effect of S1P1R activation on Ca^{2+} signalling was further confirmed in human astrocytes, where data showed the source of Ca^{2+} to be predominantly from extracellular sources. To investigate whether the effects of *p*FTY720 on S1P1R-mediated cAMP and Ca^{2+} signalling were dependent on redistribution of S1P1R, a novel biologic (MNP301), which inhibited *p*FTY720-mediated S1P1R redistribution was developed. While MNP301 prevented redistribution of S1P1Rs induced by *p*FTY720, it had no effect on continued cAMP signalling induced by *p*FTY720 but did prevent both pERK and Ca^{2+} signalling.

Internalization of S1P1Rs likely occurs via a clathrin-coated mechanism (Liu *et al.*, 1999; Watterson *et al.*, 2002). The carboxy terminus of S1P1R (ct-S1P1R) is phosphorylated by GRK2 and PKC and the successive deletion and mutation of ct-S1P1R (containing a serine-rich region ^{351}SRSKSDNSS^{359}) inhibits S1P1R phosphorylation and ligand-induced internalization (Liu *et al.*, 1999), which subsequently inhibits ubquitination and degradation of S1P1Rs (Oo *et al.*, 2007). Similar phosphorylation-dependent surface expression has also been described for the S1P3R subtype (Licht *et al.*, 2003; Rutherford *et al.*, 2005). Here, a peptide (MNP301), which comprises a Tat sequence for cell delivery fused to the last 10 amino acids of ct-S1P1R (YGRKKRRQRRR-MSSGNVNSSS) was designed and found to attenuate *p*FTY720-induced redistribution of S1P1R in astrocytes. Based on the hypothesis that the ct-S1P1R interacts with trafficking proteins which regulate receptor cycling and/or post-translational modification and that MNP301 competitively inhibits recruitment of these interacting proteins, this peptide could serve to undermine receptor trafficking, either constitutively and/or in a ligand induced manner. While the trafficking proteins interacting with S1P1Rs remain to be identified, the results here suggest a site additional to the serine-rich region (^{351}SRSKSDNSS^{359}) (Liu *et al.*, 1999) that is important for S1P1R trafficking and indicate that the extreme ct-S1P1R (^{372}MSSGNVNSSS^{382}) is equally vital to agonist-induced redistribution of the S1P1R.

Studies using HUVECs (Mullershausen *et al.*, 2009) and the current study using astrocytes suggest that *p*FTY720-induced continued signalling may be coupled with long lasting internalization. To investigate this, astrocytes were pretreated with MNP301 before addition of *p*FTY720. Notably, MNP301 did not alter *p*FTY720-mediated inhibition of forskolin-induced cAMP levels. Furthermore, despite preventing redistribution of S1P1R induced by *p*FTY720, the continued cAMP inhibition caused by *p*FTY720 was not altered by pretreatment of MNP301. The data suggested that while MNP301 prevents *p*FTY720-induced redistribution of S1P1Rs, this peptide does not affect Gi-protein mediated signalling of these receptors. The results also suggest that long lasting redistribution of S1P1R caused by *p*FTY720 is not strictly required for continued cAMP signalling in astrocytes. In other words, continued cAMP signalling may occur via either surface expressed or internalized S1P1Rs that are likely either still bound to *p*FTY720 and/or are permanently altered by *p*FTY720 treatment. Possible explanations for this finding is that *p*FTY720 induces a long lasting conformational change in S1P1R that leads to altered post-translational modification, intracellular sorting and continued signalling, thus influencing the long-term fate of the receptor.

In contrast to a continued cAMP signalling induced by *p*FTY720, this drug caused transient Ca^{2+} signalling and subsequent functional antagonism, where further stimulation of the S1P1R did not result in increased Ca^{2+} levels. Importantly the data showed that, similar to *p*FTY720, pre-treatment with S1P also inhibited further Ca^{2+} signalling, and suggesting that functional antagonism of specific S1P1R signalling pathways such as Ca^{2+} can also be caused by the natural ligand. The data also showed that MNP301 inhibited S1P1R-mediated pERK and Ca^{2+} signalling. These effects can be best explained by suggesting that MNP301 prevents interactions between adaptor proteins that ensure correct S1P1R conformation and/or regulation of second messenger proteins necessary for the propagation of both pERK and Ca^{2+} signals at the extreme ct-S1P1R.

Taken together, this study provides evidence that *p*FTY720 causes continued signalling (cAMP) and functional antagonism (Ca^{2+}) in a pathway specific manner and that these effects may be independent of S1P1R redistribution. This work also provides further insights into the effects of *p*FTY720 on S1P1R internalization and may help explain the different signalling properties of surface expressed and internalized S1P1Rs. In closing, the data suggests that transient agonism, functional antagonism or continued signalling of specific S1P1R coupled pathways induced by *p*FTY720 differ, in many cases, from the natural ligand S1P and likely explain its mechanism of action and efficacy in MS.

Acknowledgements

We are grateful to Alice Jackson and James Reynolds for experimental support. This work was supported in part by a research grants from Trinity College Dublin Ireland, Novartis Pharma Basel Switerland and The Health Research Board Ireland.

Conflict of interest

Dr. Florian Muellershausen is an employee of Novartis Pharma.

References

Bassi R, Anelli V, Giussani P, Tettamanti G, Viani P, Riboni L (2006). Sphingosine-1-phosphate is released by cerebellar astrocytes in response to bFGF and induces astrocyte proliferation through G(i)-protein-coupled receptors. Glia 53: 621–630.

Birnbaumer L (1992). Receptor-to-effector signaling through G proteins: roles for beta gamma dimers as well as alpha subunits. Cell 71: 1069–1072.

Brinkmann V, Davis MD, Heise CE, Albert R, Cottens S, Hof R *et al.* (2002). The immune modulator FTY720 targets sphingosine 1-phosphate receptors. J Biol Chem 277: 21453–21457.

Choi JW, Gardell SE, Herr DR, Rivera R, Lee CW, Noguchi K *et al.* (2011). FTY720 (fingolimod) efficacy in an animal model of multiple sclerosis requires astrocyte sphingosine 1-phosphate receptor 1 (S1P1) modulation. Proc Natl Acad Sci U S A 108: 751–756.

Dev KK, Nakajima Y, Kitano J, Braithwaite SP, Henley JM, Nakanishi S (2000). PICK1 interacts with and regulates PKC phosphorylation of mGLUR7. J Neurosci 20: 7252–7257.

Dev KK, Mullershausen F, Mattes H, Kuhn RR, Bilbe G, Hoyer D *et al.* (2008). Brain sphingosine-1-phosphate receptors: implication for FTY720 in the treatment of multiple sclerosis. Pharmacol Ther 117: 77–93.

Furukawa S, Furukawa Y (2007). [FGF-2-treatment improves locomotor function via axonal regeneration in the transected rat spinal cord]. Brain Nerve 59: 1333–1339.

Giussani P, Ferraretto A, Gravaghi C, Bassi R, Tettamanti G, Riboni L *et al.* (2007). Sphingosine-1-phosphate and calcium signaling in cerebellar astrocytes and differentiated granule cells. Neurochem Res 32: 27–37.

Goetzl EJ, Graler MH (2004). Sphingosine 1-phosphate and its type 1 G protein-coupled receptor: trophic support and functional regulation of T lymphocytes. J Leukoc Biol 76: 30–35.

Kappos L, Radue E-W, O'Connor P, Polman C, Hohlfeld R, Calabresi P *et al.* (2010). A placebo-controlled trial of oral fingolimod in relapsing multiple sclerosis. N Engl J Med 362: 1–15.

Kimura A, Ohmori T, Ohkawa R, Madoiwa S, Mimuro J, Murakami T *et al.* (2007). Essential roles of sphingosine 1-phosphate/S1P1 receptor axis in the migration of neural stem cells toward a site of spinal cord injury. Stem Cells 25: 115–124.

Licht T, Tsirulnikov L, Reuveni H, Yarnitzky T, Ben-Sasson SA (2003). Induction of pro-angiogenic signaling by a synthetic peptide derived from the second intracellular loop of S1P3 (EDG3). Blood 102: 2099–2107.

Liu CH, Thangada S, Lee MJ, Van Brocklyn JR, Spiegel S, Hla T (1999). Ligand-induced trafficking of the sphingosine-1-phosphate receptor EDG-1. Mol Biol Cell 10: 1179–1190.

Malchinkhuu E, Sato K, Muraki T, Ishikawa K, Kuwabara A, Okajima F (2003). Assessment of the role of sphingosine 1-phosphate and its receptors in high-density lipoprotein-induced stimulation of astroglial cell function. Biochem J 370 (Pt 3): 817–827.

Meno-Tetang GM, Li H, Mis S, Pyszczynski N, Heining P, Lowe P *et al.* (2006). Physiologically based pharmacokinetic modeling of FTY720 (2-amino-2[2-(-4-octylphenyl)ethyl]propane-1,3-diol hydrochloride) in rats after oral and intravenous doses. Drug Metab Dispos 34: 1480–1487.

Mullershausen F, Craveiro LM, Shin Y, Cortes-Cros M, Bassilana F, Osinde M *et al.* (2007). Phosphorylated FTY720 promotes astrocyte migration through sphingosine-1-phosphate receptors. J Neurochem 102: 1151–1161.

Mullershausen F, Zecri F, Cetin C, Billich A, Guerini D, Seuwen K (2009). Persistent signaling induced by FTY720-phosphate is mediated by internalized S1P1 receptors. Nat Chem Biol 5: 428–434.

Novgorodov AS, El-Alwani M, Bielawski J, Obeid LM, Gudz TI (2007). Activation of sphingosine-1-phosphate receptor S1P5 inhibits oligodendrocyte progenitor migration. FASEB J 21: 1503–1514.

Oo ML, Thangada S, Wu MT, Liu CH, Macdonald TL, Lynch KR *et al.* (2007). Immunosuppressive and anti-angiogenic sphingosine 1-phosphate receptor-1 agonists induce ubiquitinylation and proteasomal degradation of the receptor. J Biol Chem 282: 9082–9089.

Osinde M, Mullershausen F, Dev KK (2007). Phosphorylated FTY720 stimulates ERK phosphorylation in astrocytes via S1P receptors. Neuropharmacology 52: 1210–1218.

Pebay A, Toutant M, Premont J, Calvo CF, Venance L, Cordier J *et al*. (2001). Sphingosine-1-phosphate induces proliferation of astrocytes: regulation by intracellular signalling cascades. Eur J Neurosci 13: 2067–2076.

Rao TS, Lariosa-Willingham KD, Lin FF, Palfreyman EL, Yu NC, Chun J *et al*. (2003). Pharmacological characterization of lysophospholipid receptor signal transduction pathways in rat cerebrocortical astrocytes. Brain Res 990: 182–194.

Riboni L, Viani P, Bassi R, Giussani P, Tettamanti G (2001). Basic fibroblast growth factor-induced proliferation of primary astrocytes. evidence for the involvement of sphingomyelin biosynthesis. J Biol Chem 276: 12797–12804.

Rouach N, Pebay A, Meme W, Cordier J, Ezan P, Etienne E *et al*. (2006). S1P inhibits gap junctions in astrocytes: involvement of G and Rho GTPase/ROCK. Eur J Neurosci 23: 1453–1464.

Rutherford C, Ord-Shrimpton FU, Sands WA, Pediani JD, Benovic JL, McGrath JC *et al*. (2005). Phosphorylation-independent internalisation and desensitisation of the human sphingosine-1-phosphate receptor S1P3. Cell Signal 17: 997–1009.

Salomon Y (1979). Adenylate cyclase assay. Adv Cyclic Nucleotide Res 10: 35–55.

Sato M, Dobashi H, Ohye H, Akiyama T, Kawanishi J, Kaji Y *et al*. (1999). Effect of growth hormone on growth failure and bone loss induced by supraphysiologic dose of glucocorticoid in rats. Endocr J 46 (Suppl.): S89–S92.

Sheridan GK, Dev KK (2012). S1P1 receptor subtype inhibits demyelination and regulates chemokine release in cerebellar slice cultures. Glia 60: 382–392.

Sorensen SD, Nicole O, Peavy RD, Montoya LM, Lee CJ, Murphy TJ *et al*. (2003). Common signaling pathways link activation of murine PAR-1, LPA, and S1P receptors to proliferation of astrocytes. Mol Pharmacol 64: 1199–1209.

Watterson KR, Johnston E, Chalmers C, Pronin A, Cook SJ, Benovic JL *et al*. (2002). Dual regulation of EDG1/S1P(1) receptor phosphorylation and internalization by protein kinase C and G-protein-coupled receptor kinase 2. J Biol Chem 277: 5767–5777.

Wu YP, Mizugishi K, Bektas M, Sandhoff R, Proia RL (2008). Sphingosine kinase 1/S1P receptor signaling axis controls glial proliferation in mice with Sandhoff disease. Hum Mol Genet 17: 2257–2264.

Yamagata K, Tagami M, Torii Y, Takenaga F, Tsumagari S, Itoh S *et al*. (2003). Sphingosine 1-phosphate induces the production of glial cell line-derived neurotrophic factor and cellular proliferation in astrocytes. Glia 41: 199–206.

Zhang Z, Fauser U, Schluesener HJ (2008). Early attenuation of lesional interleukin-16 up-regulation by dexamethasone and FTY720 in experimental traumatic brain injury. Neuropathol Appl Neurobiol 34: 330–339.